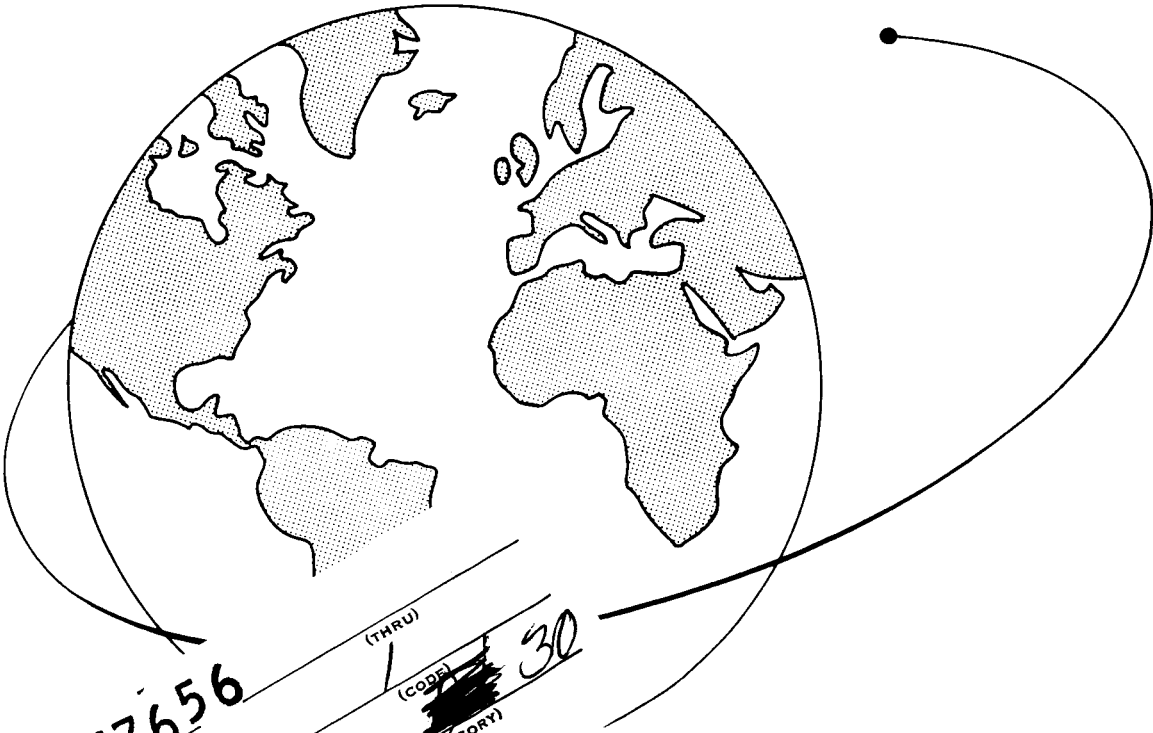


# DESIGN OF A SATELLITE EXPERIMENT FOR ATMOSPHERIC DENSITY AND NEAR-FREE-MOLECULE-FLOW AERODYNAMICS

L.S. LAM, G.M. MENDES and C.A. LUNDQUIST



N67-37656  
 (ACCESSION NUMBER)  
 46  
 (PAGES)  
 CR# 88868  
 (NASA CR OR TMX OR AD NUMBER)

(THRU) 1  
 (CODE) ~~30~~  
 (CATEGORY) 30

Smithsonian Astrophysical Observatory  
SPECIAL REPORT 241

Research in Space Science  
SAO Special Report No. 241

DESIGN OF A SATELLITE EXPERIMENT  
FOR ATMOSPHERIC DENSITY AND NEAR-FREE-MOLECULE-FLOW  
AERODYNAMICS

Louisa S. Lam, Geraldine M. Mendes, and Charles A. Lundquist

June 5, 1967

Smithsonian Institution  
Astrophysical Observatory  
Cambridge, Massachusetts, 02138

## TABLE OF CONTENTS

<u>Section</u>		<u>Page</u>
	ABSTRACT . . . . .	v
1	INTRODUCTION . . . . .	1
2	AERODYNAMIC-DRAG REPRESENTATION . . . . .	3
3	ORBIT CHANGES RESULTING FROM DRAG . . . . .	7
4	CONCEPT OF EXPERIMENT . . . . .	9
5	EXTENDED EXPERIMENT . . . . .	12
6	TEMPORAL VARIATION OF THE ATMOSPHERE . . . . .	14
7	SURFACE PREPARATION . . . . .	15
8	REPRESENTATION OF THE GEOPOTENTIAL . . . . .	16
9	OBSERVATION AND DATA PROCESSING . . . . .	18
10	EXPERIMENT REQUIREMENTS . . . . .	20
11	EXAMPLE 1, SCOUT LAUNCH VEHICLE . . . . .	21
12	EXAMPLE 2, SATURN SECONDARY EXPERIMENT . . . . .	29
13	CONCLUSIONS . . . . .	35
14	REFERENCES . . . . .	36
	BIOGRAPHICAL NOTES . . . . .	39

## LIST OF ILLUSTRATIONS

<u>Figure</u>		<u>Page</u>
1	Predicted values for example of Scout-launched satellites	23
2	$\Delta M/t^2$ versus apogee for the example of Scout-launched satellites. . . . .	24
3	Separation as a function of apogee, for example of Scout-launched satellites. . . . .	27
4	(a) $\frac{dP(2)}{dt} - \frac{dP(1)}{dt}$ versus apogee for the example of Saturn-launched satellites	
	(b) $\frac{dP(3)}{dt} - \frac{dP(1)}{dt}$ versus apogee for the example of Saturn-launched satellites. D(1) = 20 cm; D(2) = 60 cm; D(3) = 100 cm . . . . .	31
5	Curves for the example of Saturn-launched satellites. $\frac{\Delta M}{t^2}$ versus apogee for: (a) sphere 2 from sphere 1, and (b) sphere 3 from sphere 1 . . . . .	32
6	Angular separation of sphere 2 from sphere 1 at apogee 2000 km versus time, for Saturn-launched satellites. . . . .	33
7	Angular separation of sphere 3 from sphere 1 at apogee 2000 km versus time, for Saturn-launched satellites. . . . .	34

LIST OF TABLES

<u>Table</u>		<u>Page</u>
1	Drag coefficient for 1-m-diameter sphere . . . . .	6
2	Orbital parameters at apogee 2400 km . . . . .	26
3	Orbital parameters at apogee 4000 km . . . . .	28
4	Nominal parameters for Saturn secondary experiment . . . . .	29

## ABSTRACT

The atmospheric drag on a satellite is conveniently determined from the rate of change of the orbital period  $dP/dt$ . This procedure can be extended to the near-free-molecule-flow regime, in which the drag coefficient of a sphere is expressed by  $C_D = C_{Dfm} - F(S_b, S_\infty)/K$ , where  $C_{Dfm}$  is the free-molecule-flow coefficient, and  $F(S_b, S_\infty)$  is a function of the molecular speed ratios for gas diffusely emitted from the body surface and for the free stream. The free-stream Knudsen number  $K$  can be expressed as  $1/K = BD\rho$ , where  $D$  is the sphere diameter,  $\rho$  is the atmospheric density, and  $B$  is a constant. In terms of the usual orbital elements and the density at perigee  $\rho_P$ ,

$$dP/dt = -3a \left( \frac{A}{m} \right) \left( f_1 C_{Dfm} \rho_P - f_2 BD F \rho_P^2 \right) ,$$

where

$$f_i = \int_0^\pi \left( \frac{\rho}{\rho_P} \right)^i \frac{(1 + e \cos E)^{3/2}}{(1 - e \cos E)^{1/2}} dE .$$

From the measured  $dP/dt$  for two or more satellites with nearly identical  $A/m$  and orbits, it would be possible to find the atmospheric density at low altitude and a value of  $F$  for comparison with theory.

For a practical experiment, particular orbit characteristics and satellite parameters must be selected to match available launch-vehicle performance. Two concrete examples are discussed. The first assumes the performance of the Scout vehicle. This example shows that a reasonable experiment seems possible even for this modest vehicle. The second example adopts parameters that may be typical of a secondary mission on a Saturn class vehicle.

DESIGN OF A SATELLITE EXPERIMENT  
FOR ATMOSPHERIC DENSITY AND NEAR-FREE-MOLECULE-FLOW  
AERODYNAMICS

Louisa S. Lam, Geraldine M. Mendes, and Charles A. Lundquist

1. INTRODUCTION

Accurate tracking of artificial satellites has provided a powerful method for studying the several phenomena that result in forces acting on an orbiting body. Meticulous analyses of satellite positions have produced a detailed representation of the earth's gravitational potential (Gaposchkin, 1966a, 1967; Kozai, 1964, 1966) and models for the atmospheric density and its variation (Jacchia, 1965). Most of the atmospheric information obtained this way pertains to altitudes above 200 km. It is natural to inquire how established procedures can be extended to study the atmosphere and aerodynamic phenomena at lower altitudes for which departures from free-molecule-flow aerodynamics are significant for bodies of practical dimension. These altitudes are below those where satellites usually persist for appreciable lifetimes.

Within the possibilities of present technology, reasonable experiments can be designed that will yield both a measurement of atmospheric density and experimental data on the drag coefficient of a sphere in near-free-molecule flow. This dual objective is natural, even inevitable, since the aerodynamic forces determined from resulting satellite accelerations, of course, depend upon both the atmospheric density and the details of the interaction of the satellite with the atmosphere.

---

This work was supported in part by NsG 87-60 from the National Aeronautics and Space Administration.

The suggested experiments require that a single rocket vehicle launch an ensemble of two or more spherical satellites into essentially identical orbits. These bodies would be similar in most of their characteristics, but would differ in those that allow a separation and an identification of the factors that enter into the aerodynamic drag.

In arriving at a practical experiment, we must recognize the satellite-tracking accuracy currently attainable. The accuracy obtained with the existing network of Baker-Nunn cameras has been assumed.

## 2. AERODYNAMIC-DRAG REPRESENTATION

To design the experiment, we must adopt a representation of the drag coefficient for near-free-molecule flow. The choice is somewhat subjective, since several formulas have been suggested by different authors. Fortunately, some of the earlier differences between theory and laboratory results have been resolved in later papers (Maslach, Willis, Tang, and Ko, 1964). Nevertheless, further data of the sort obtainable from a satellite experiment would be particularly valuable to compare with theory for parameter values, such as large Knudsen numbers, difficult to attain in the laboratory.

Most of the theoretical expressions for the near-free-molecule-flow drag coefficient of a sphere have the form (Maslach et al., 1964)

$$C_D = C_{Dfm} - \frac{1}{K} F(S_b, S_\infty) \quad , \quad (1)$$

where  $C_{Dfm}$  is the value of the drag coefficient for free-molecule flow,  $K$  is the free-stream Knudsen number (free-stream mean free path/sphere diameter),  $S_b$  is the molecular speed ratio of the gas diffusely emitted from the surface, and  $S_\infty$  is the molecular speed ratio for the free stream. For this discussion, we can represent the last three quantities by the following equations:

$$K = \frac{w}{\sqrt{2} \pi N_0 \sigma^2 \rho D} \quad , \quad (2)$$

$$S_b = \frac{U}{\sqrt{2 RT_b/w}} \quad , \quad (3)$$

and

$$S_{\infty} = \frac{U}{\sqrt{2RT_{\infty}/w}} \quad , \quad (4)$$

where  $D$  is the sphere diameter,  $\rho$  is the atmospheric density,  $w$  is the mean molecular weight of the air molecules,  $N_0$  is Avogadro's number ( $N_0 = 6.02 \times 10^{23}$  atoms/g mole),  $\sigma$  is the effective collision diameter of a molecule of air,  $T_b$  is the surface temperature of the orbiting body,  $T_{\infty}$  is the temperature of the atmosphere,  $U$  is the satellite velocity relative to the atmosphere, and  $R$  is the gas constant per mole ( $R = 8.3170 \times 10^7$  erg/mole °K). In this same notation, for diffuse reflection (Schaaf and Chambré, 1958),

$$C_{Dfm} = 2 + \frac{1.18}{S_b} \quad . \quad (5)$$

Different forms of the function  $F(S_b, S_{\infty})$  have been derived by various authors using different procedures (Maslach et al., 1964):

$$\text{(Baker and Charwat)} \quad F = 0.24 S_b + 1.06 \quad , \quad (6a)$$

$$\text{(Willis)} \quad F = \frac{0.165 S_b + 1.44 - 1.13/S_b}{S_{\infty}} \quad , \quad (6b)$$

$$\text{(Rose)} \quad F = \frac{0.33 S_b - 0.12}{S_{\infty}} \quad . \quad (6c)$$

In their review of this topic, Maslach et al. conclude that the last two expressions give the best agreement with laboratory data.

Using equation (2) to express  $1/K$  in terms of  $\rho$ ,  $w$ , and  $D$ , we get a representation of the aerodynamic drag per unit mass of the satellite:

$$\frac{\text{drag}}{\text{unit mass}} = \frac{1}{2} C_D \frac{A}{m} U^2 \rho = \frac{1}{2} \left[ C_{Dfm} - BF(S_b, S_\infty) D \rho \right] \frac{A}{m} \rho U^2 \quad , \quad (7)$$

where  $A$  is the cross-section area of the sphere,  $m$  is the mass of the sphere, and

$$B = \frac{\sqrt{2} \pi \sigma^2 N_0}{w} \quad .$$

For the purpose of the experiment under discussion, we can consider several of the quantities in this representation to be known. The velocity of the satellite can be found from the orbital elements obtained by tracking the satellite. The surface temperature of the sphere can be calculated using proved techniques (e. g., Heller, 1961). The mean molecular weight and the effective collision diameter of the air molecules vary quite slowly with altitude in the interval of interest, and appropriate values from the literature can be used ( $\sigma = 3.65 \times 10^{-10}$  m). The diameter and mass of the sphere are parameters to be adjusted in the design of the experiment, but will be known quantities for an actual body.

If equation (5) is accepted as correct, only the atmospheric density  $\rho$  and the values of  $F(S_b, S_\infty)$  remain to be determined from appropriate analysis of tracking data. The value of  $\rho$  is of obvious geophysical interest. The experimental values of  $F(S_b, S_\infty)$  are valuable for comparison with theoretical values derived by various procedures (equations (6)).

To estimate the magnitude of the second term of equation (7) relative to the first term, we can use the theoretical expressions for  $F$  with values of  $\rho$  from a standard atmosphere (Jacchia, 1965). Values for equation (6b) are shown in Table 1.

Table 1. Drag coefficient for 1-m-diameter sphere\*

Altitude (km)	K	$B F(S_b, S_\infty) D_\rho$	$C_{Dfm}$	$C_D$
120	3.1	0.084	2.062	1.978
130	9.4	0.035	2.063	2.028
140	19.2	0.019	2.063	2.044
150	32.6	0.012	2.064	2.051
160	50.2	0.009	2.064	2.056
170	72.2	0.006	2.065	2.059

\*The following values are used in the table:  
 atmospheric model from Jacchia (1965) with exospheric  
 temperature = 1300°K,  
 F is given by equation (6b),  
 $T_b = 300^\circ \text{K}$ ,  
 $U = 8.2 \text{ km/sec}$ .

### 3. ORBIT CHANGES RESULTING FROM DRAG

The effect of atmospheric drag on the anomalistic period  $P$  of a satellite has been conveniently expressed by Sterne (1958). If the rotation of the atmosphere is neglected, the rate of change of the period is

$$\frac{\Delta P}{P} = \frac{dP}{dt} = -\frac{3}{2} \frac{A}{m} \rho_P a \int_0^{2\pi} C_D \frac{\rho}{\rho_P} \frac{(1 + e \cos E)^{3/2}}{(1 - e \cos E)^{1/2}} dE \quad , \quad (8)$$

where  $\rho_P$  is the density at perigee,  $a$  the semimajor axis,  $e$  the eccentricity, and  $E$  the eccentric anomaly. As explained by Jacchia (1963), this equation is the usual starting place for determinations of atmospheric density because the period and its changes are rather directly obtained from tracking data.

To simplify notation, it is convenient to define quantities  $f_1$  and  $f_2$  by

$$f_1 = \int_0^{\pi} \frac{\rho}{\rho_P} \frac{(1 + e \cos E)^{3/2}}{(1 - e \cos E)^{1/2}} dE \quad (9)$$

and

$$f_2 = \int_0^{\pi} \left( \frac{\rho}{\rho_P} \right)^2 \frac{(1 + e \cos E)^{3/2}}{(1 - e \cos E)^{1/2}} dE \quad . \quad (10)$$

Tables of  $f_1$  are given by Jacchia and Slowey (1963a) and similar tables of  $f_2$  are easily constructed. Using this notation and the adopted expression for  $C_D$  in equation (8) gives (Lundquist, 1967)

$$\frac{dP}{dt} = - 3 a f_1 \frac{A}{m} C_{Dfm} \rho_P + 3 a f_2 B \frac{A}{m} D F \rho_P^2 . \quad (11)$$

In this equation,  $B$  has been treated as a constant because it varies much more slowly with altitude than does  $\rho$ .

#### 4. CONCEPT OF EXPERIMENT

To investigate near-free-molecule-flow aerodynamics and atmospheric density at low altitudes, we suggest two spherical satellites having identical  $A/m$  and having surface preparations that ensure equal surface temperatures. These spheres should be launched by the same vehicle into initial orbits as nearly identical as practical. The diameter of one sphere,  $D(1)$ , should be as small as possible and still allow reliable photographic tracking with the Baker-Nunn cameras. The diameter of the second,  $D(2)$ , should be as large as can be contained within the available launch vehicle. Using simple procedures discussed below, values for the rate of change of the periods  $P(1)$  and  $P(2)$  can be obtained from tracking data. For two satellites under these conditions, equation (11) gives two linear simultaneous equations (12) and (13) for unknowns  $C_{Dfm} \rho_P$  and  $BF\rho_P^2$ . The coefficients multiplying these unknowns involve only quantities known a priori or determined from tracking data. The quantities  $f_1$  and  $f_2$  are functions of the atmospheric scale height near perigee, as well as of the orbital elements, but the value of the scale height can be estimated with sufficient accuracy for computing  $f_1$  and  $f_2$ :

$$\left[ -3 af_1 \frac{A}{m} \right] C_{Dfm} \rho_P + \left[ 3 af_2 D(1) \frac{A}{m} \right] BF\rho_P^2 = \frac{dP(1)}{dt} \quad (12)$$

and

$$\left[ -3 af_1 \frac{A}{m} \right] C_{Dfm} \rho_P + \left[ 3 af_2 D(2) \frac{A}{m} \right] BF\rho_P^2 = \frac{dP(2)}{dt} \quad (13)$$

Under the assumption that the orbits are identical, these have the simple solutions

$$C_{Dfm} \rho_P = \frac{1}{\left(3 a f_1 \frac{A}{m}\right) [D(2) - D(1)]} \left[ D(1) \frac{dP(2)}{dt} - D(2) \frac{dP(1)}{dt} \right] \quad (14)$$

and

$$BF \rho_P^2 = \frac{1}{\left(3 a f_2 \frac{A}{m}\right) [D(2) - D(1)]} \left[ \frac{dP(2)}{dt} - \frac{dP(1)}{dt} \right] \quad (15)$$

If the perigee altitude were above the near-free-molecule-flow region for the adopted satellite diameters, the periods would have the same rate of change and equation (14) would reduce to the usual expression applied to determine  $C_{Dfm} \rho_P$ . Thus equation (14) is only the familiar expression with a simple correction for the case of near-free-molecule flow. If a value of  $C_{Dfm}$  is accepted from equation (5) or from some other source (Cook, 1965), equation (14) yields a value for  $\rho_P$ . Using this value for  $\rho_P$  with equation (15) gives a value for BF, which is a measure of the departure from free-molecule-flow aerodynamics. If B is considered known, a value of F follows immediately.

The accuracy with which F is obtained depends critically upon the selection of satellite and orbit parameters such that the rates of change of the periods differ significantly. Variation of  $\rho_P$  during the interval of observation can also limit the accuracy obtained.

Equations (14) and (15) are intended only to illustrate the principal features of the analysis. For example, as the satellites separate, the assumption of identical orbits begins to break down; however, first-order corrections for this can be introduced. The effects of an initial separation

velocity between the spheres and the rotation of the atmosphere can likewise be incorporated.

Introducing into the experiment a third sphere, again with the same  $A/m$  but with a still different diameter,  $D(3)$ , would provide a useful check on the results. A third equation of the form (12) is not independent, but it must be consistent with (12) and (13). A demonstration of the required consistency would lend substantial credence to the solution. This is particularly true because equations (12) and (13) will always have a solution, but this solution is by no means guaranteed to be meaningful, as it assumes equation (1) is correct. Given three or more equations of the form of (12) with reasonable consistency, a least-squares solution can be obtained replacing equations (14) and (15).

On the other hand, there is some reason to believe that a term proportional to  $(D \rho_P)^2$  should be added to equation (1) (Sherman, Willis, and Maslach, 1964). If this should be necessary, equation (11) would have a corresponding additional term involving  $\rho_P^3$ ,  $f_3$ , and a coefficient characterizing the importance of this added term. Data on three spheres of different size then would be required to investigate the departure from free-molecule-flow aerodynamics, but otherwise the same procedures could be followed.

## 5. EXTENDED EXPERIMENT

The simple experiment sketched in the previous section can be extended to alleviate the weaknesses that result because the orbits become different as the spheres separate. This is accomplished by adjusting slightly the masses and hence the  $A/m$  ratios to just balance the expected drag differences caused initially by departure from free-molecule-flow aerodynamics. For the two-sphere case, this requires that  $(A/m)(1)$  and  $(A/m)(2)$  be chosen so that

$$\frac{dP(1)}{dt} = \frac{dP(2)}{dt} \quad (16)$$

This implies that

$$\frac{\frac{A}{m}(1)}{\frac{A}{m}(2)} = \frac{f_1 C_{Dfm} - f_2 D(2) BF \rho_P}{f_1 C_{Dfm} - f_2 D(1) BF \rho_P} \quad (17)$$

Because  $BF$  and  $\rho_P$  are imperfectly known, equation (17) cannot be exactly satisfied; however, the best estimates of these can be used to achieve a first approximation. Also, as the eccentricities of the orbits decrease, the values of  $f_1$  and  $f_2$  change, which may generate a departure from equation (17).

Corresponding to equations (14) and (15) for this generalized case are the equations

$$C_{Dfm} \rho_P = \frac{1}{\left[ 3 a f_1 \frac{A}{m}(1) \frac{A}{m}(2) \right] [D(2) - D(1)]} \left[ D(1) \frac{A}{m}(1) \frac{dP(2)}{dt} - D(2) \frac{A}{m}(2) \frac{dP(1)}{dt} \right] \quad (18)$$

and

$$BF\rho_P^2 = \frac{1}{\left[3 \text{af}_2 \frac{A}{m}(1) \frac{A}{m}(2)\right] [D(2) - D(1)]} \left[ \frac{A}{m}(1) \frac{dP(2)}{dt} - \frac{A}{m}(2) \frac{dP(1)}{dt} \right] . \quad (19)$$

Perhaps it is worth noting that these equations are meaningful whether or not equation (17) is satisfied.

In the following discussions and examples, the point of view of the previous section will be retained because the spatial separation of the spheres is an easily pictured measure of the observability of the desired quantities. However, an actual execution of the experiment would probably employ the more general approach of this section.

## 6. TEMPORAL VARIATION OF THE ATMOSPHERE

Changes of atmospheric density as a function of time, are well known above 200 km, but less is known of their magnitude at lower altitudes (Jacobs, 1967). Measurements of changes that may occur are as interesting as determinations of the density. An investigation of temporal phenomena would be facilitated by the inclusion of a very heavy sphere in the ensemble. This sphere could have the same size and surface preparation as one of the other spheres, but it should have as great a mass as practical.

The high-density body will remain in orbit longer than the lighter bodies in the aerodynamics experiment. The knowledge of the drag coefficient generated in the initial phases of the experiment is directly applicable to the later history of the heavy body. An analysis of the orbit of the long-lived satellite in the usual way is useful in the measurement of the variation of atmospheric density as a function of time and of solar and geophysical events.

## 7. SURFACE PREPARATION

In the adopted expressions for the drag coefficient, the properties of the surface enter through  $S_b$ , the ratio of the orbital speed to the speed with which gas molecules are diffusely emitted from the surface. The latter speed depends upon phenomena at the surface of the satellite. The expression for  $S_b$  given in equation (3) is an approximation for more involved theories that could be invoked. For example, the relation between the surface temperature and the velocity of emitted molecules is often characterized by an accommodation coefficient (Wachman, 1962; Springer and Tsai, 1964).

For the initial experiment considered here, the most important requirements are that the spheres be carefully prepared with identical surface characteristics with respect to velocity of emitted molecules, and that the surface temperatures be equal. It is hoped that these conditions are not contradictory. These requirements have been assumed in the description of the experiment. Alternatively, the theory of the experiment might be slightly modified to include a correction for unavoidable differences in surface properties.

The usefulness of the experiment can be enhanced if the surface preparation is one that has been studied by laboratories investigating the relevant surface phenomena. Information from such studies will be valuable in the selection of an appropriate surface material and preparation.

If vehicle performance would allow additional satellites, an experiment with spheres differing only in their surface characteristics could be envisioned, and the data obtained could be compared with predictions from theory. There is little reason, however, to perform such an experiment at very low-perigee altitudes, unless the objective were a study of the dependence of  $F$  on  $S_b$ . The latter would presuppose an adequate evaluation of  $S_b$  and the dependence of  $C_{Dfm}$  upon it.

## 8. REPRESENTATION OF THE GEOPOTENTIAL

The determination of accurate orbits for the satellites in the suggested experiment depends upon an adequate representation of the geopotential. Fortunately, the philosophy of the experiment minimizes the demands on the geopotential representation. Because the perigee of the suggested satellites will be quite low, and if the eccentricity is not too great, the effect of high-order harmonics in the gravitational field may be greater than that experienced by satellites in more distant orbits. Thus the adopted standard representation of the geopotential may not account for all detectable gravitational perturbations on an individual satellite. This may introduce an increased "noise level" in the orbit-determination process.

If this should become troublesome, the same dense sphere used for temporal atmospheric variation also may relieve this problem. If the additional sphere is denoted by 4, then from equation (8),

$$\frac{dP(4)}{dt} = \frac{m(1)}{m(4)} \frac{dP(1)}{dt} \quad (20)$$

If, further,  $m(4)$  is significantly larger than  $m(1)$ , perhaps by a factor of 5 or 10, then equation (20) provides accurate values of  $dP(4)/dt$  from the larger, more easily measured values of  $dP(1)/dt$ .

A similar situation prevails for the drag-induced changes in the other orbital elements of sphere 4. These can be expressed with relatively greater accuracy from the drag measured by sphere 1. But the drag on sphere 4 is already relatively small because  $A/m$  is small. Hence, the uncertainty associated with drag on sphere 4 is something like  $m(1)/m(4)$  less than that on sphere 1.

Drag corrections derived from sphere 1 can be applied to the orbit of sphere 4, and this orbit examined for the adequacy of the adopted geopotential. If the residuals between observation and calculation approach the accuracy of the observations, then the adequacy of the geopotential is strongly verified. In this case, the analysis of atmospheric effects on the light satellites can proceed with assurance that the "noise" induced by uncertainty in the geopotential is small. Asking that the residuals approach the observational accuracy is probably too stringent. Presumably, the geopotential is sufficient if the residuals of the corrected orbit for sphere 4 are small compared to the uncertainty in the determination of the separations induced by differences in  $C_D$  for the high-drag spheres.

If the residuals for the corrected orbit of sphere 4 are greater than expected, the orbit can perhaps provide information for an improved determination of the geopotential. In an imprecise sense, the corrected orbit is a low-perigee, drag-free orbit.

## 9. OBSERVATION AND DATA PROCESSING

The Baker-Nunn cameras and associated timing systems produce fundamental data in the form of station-to-satellite directions accurate to 2 to 3 arcsec and associated observation times accurate to 1 msec. The station positions are known globally to an accuracy of 10 to 20 m (Köhnlein, 1966, 1967). The observations and station positions are used in a differential orbit improvement (DOI) program to obtain an orbit for the satellite observed (Veis and Moore, 1960; Gaposchkin, 1966b). This program uses a standard set of station coordinates and coefficients for the spherical harmonic representation of the earth's gravitational field (those currently used are from the Smithsonian Institution 1966 Standard Earth (Lundquist and Veis, 1966)). It also takes into account the lunar perturbations and various minor corrections. For a satellite on which drag is insignificant, the mean residual between observation and calculation is typically around 4 arcsec, which approaches the accuracy of the fundamental observations.

When used on a satellite with appreciable drag, the DOI program gives a series representation for the orbital elements, including mean anomaly, in which the most significant remaining effect is that due to atmospheric drag. For the mean anomaly  $M$  this series is usually expressed in the form

$$M = M_0 + M_1 t + M_2 t^2 + \dots, \quad (21)$$

where  $M_i$  are constants determined by the DOI program, and  $t$  is the time interval from some initial time. This is the form in which SAO publishes satellite orbital elements. In principle,  $dP/dt$  due to drag may be obtained directly from

$$\frac{dP}{dt} = - \frac{\ddot{M}}{\dot{M}^2}. \quad (22)$$

In practice, a more refined but conceptually equivalent procedure is actually used (Jacchia and Slowey, 1963b). The values obtained are available for use with equations (14) and (15), or with (18) and (19).

## 10. EXPERIMENT REQUIREMENTS

For a practical experiment, particular orbit characteristics and satellite parameters must be selected to match available launch-vehicle performance. Two concrete examples will be discussed. The first assumes the performance of the Scout vehicle. This example shows that a reasonable experiment seems possible even for this modest vehicle. The second example adopts parameters that may be typical of a secondary mission on a Saturn class vehicle.

In the Scout example, only two spheres are considered, recognizing the vehicle limitations. In the second example, three spheres are suggested for the aerodynamic experiment and a fourth sphere is included to monitor time variations of the atmosphere and to verify the geopotential representation.

## 11. EXAMPLE 1, SCOUT LAUNCH VEHICLE

For this example the performance of the Scout vehicle is adopted (National Aeronautics and Space Administration, 1966). Within necessary constraints, the objective is to define an optimum experiment. The first constraint, imposed by the philosophy of the experiment, requires that the two spheres have equal area-to-mass ratios, so that

$$\frac{D(1)^2}{m(1)} = \frac{D(2)^2}{m(2)} \quad . \quad (23)$$

For an orbit yet to be specified, the sum of the two masses must correspond to  $m$ , the Scout payload capability less an allowance for support structure,

$$m(1) + m(2) = m \quad . \quad (24)$$

The diameter  $D(2)$  of the larger sphere will be fixed at the maximum diameter that can be contained within the Scout payload area. This is about 76 cm (National Aeronautics and Space Administration, 1966):

$$D(2) = 76 \text{ cm} \quad . \quad (25)$$

To ensure that the small sphere can be tracked with the Baker-Nunn camera, a minimum diameter must be imposed. This minimum depends upon the maximum distance to the satellite. This condition can be expressed as a function of the apogee distance  $r_A$  and the radius of the earth  $r_E$ :

$$D(1) = 10^{-7} (r_A - r_E) \quad . \quad (26)$$

A linear relationship between diameter and range follows from the usual expressions for illumination from a satellite as a function of diameter and radius (Veis, 1965; Zirker, Whipple, and Davis, 1956). The factor  $10^{-7}$  is a threshold based on experience with the Baker-Nunn camera. A more conservative value would be  $1.4 \times 10^{-7}$ .

Combining (23) through (26) gives  $m(1)$ ,  $m(2)$ ,  $D(1)$ , and  $D(2)$  as functions of the parameters related to the vehicle performance, i.e.,  $m$ ,  $r_P$ , and  $r_A$ . For an eastward launch from Wallops Island, Scout performance data are available as a family of curves of apogee versus payload for a sequence of perigee values. Hence, for various values of  $r_P$  and  $r_A$ , a value of  $m$  is obtained, and consequently values of  $m(1)$ ,  $m(2)$ ,  $D(1)$ , and  $D(2)$  can be calculated.

A set of these can be used with a theoretical value of  $F$  and a nominal value of  $\rho_P$  in equation (15) to predict a value for  $[dP(2)/dt] - [dP(1)/dt]$ . Curves obtained this way are shown in Figure 1. The Jacchia (1965) model atmosphere with an exospheric temperature equal to 1300°K has been used for these and subsequent examples.

The difference in the rate of change of the periods is a measure of the detectability of the departure from free-molecule-flow aerodynamics. A more easily interpreted measure is the separation of the two satellites after some time interval. This can be estimated starting with equations (12) and (13) and using the theoretical values of the required parameters. Assuming for this estimate that there is negligible initial separation velocity, the expected separation in mean anomaly can be estimated by the equation

$$\Delta M = \frac{1}{\bar{P}^2} \frac{3}{2} FB \frac{A}{m} \rho_P^2 \text{af}_2 [D(2) - D(1)] t^2, \quad (27)$$

where  $\Delta M$  is in revolutions, and  $\bar{P}$  is the mean period of the two satellites for the interval  $t$  since launch.

If the atmospheric density at a particular altitude is an objective of the experiment, this altitude determines  $r_P$ . In this case, the corresponding curve in Figure 1 shows the range of obtainable  $r_A$  and  $[dP(2)/dt] - [dP(1)/dt]$ , still assuming Scout performance. Equation (27) can be used to estimate the separation of the satellites as a function of time. In Figure 2, the factor multiplying  $t^2$  on the right side of equation (27) is plotted for various values of  $r_P$  and  $r_A$ . The initial value of  $P$  has been used for  $\bar{P}$ . Recognizing this conservative approximation, the separation at time  $t$  after launch can be found.

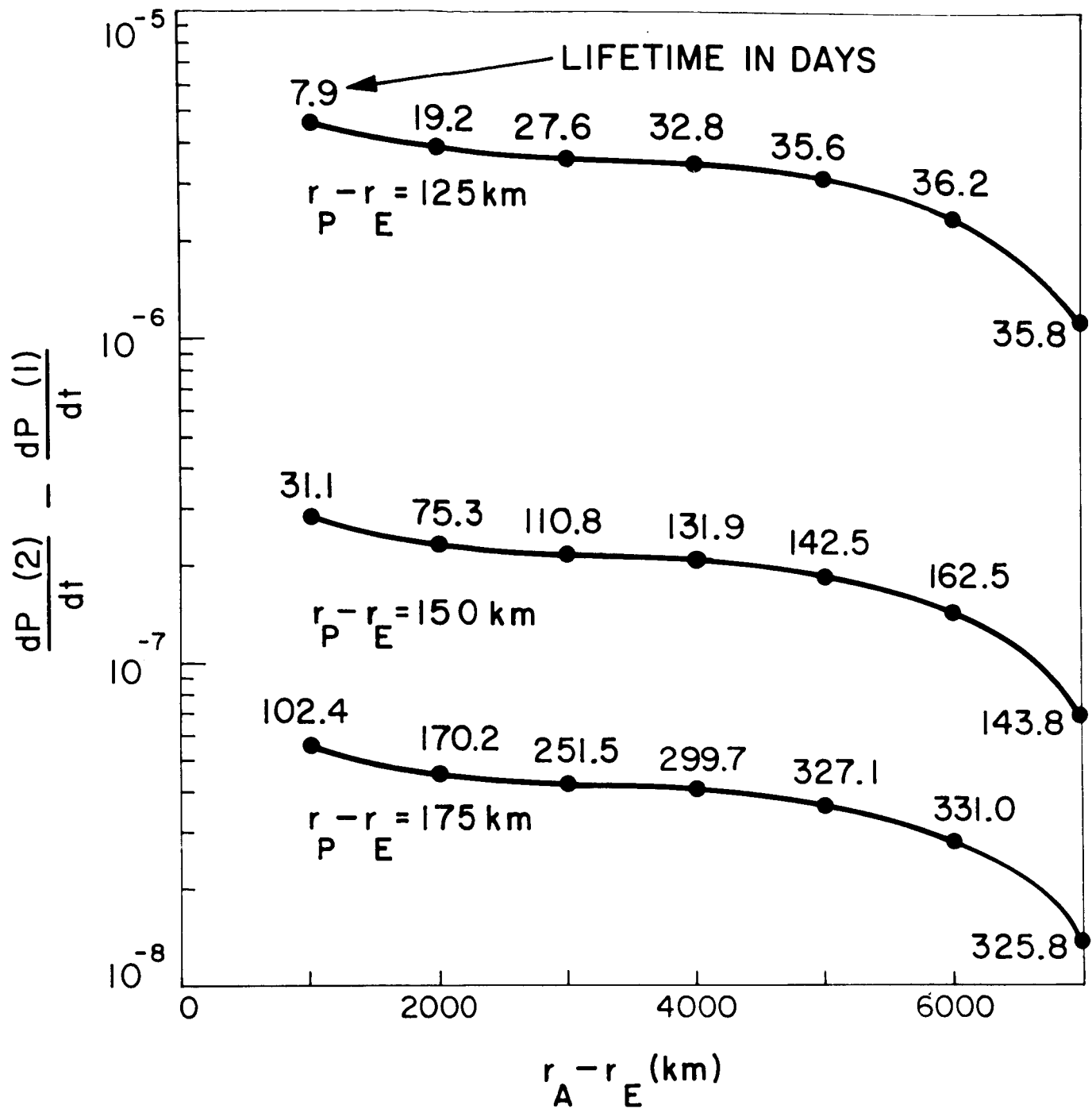


Figure 1. Predicted values for example of Scout-launched satellites.

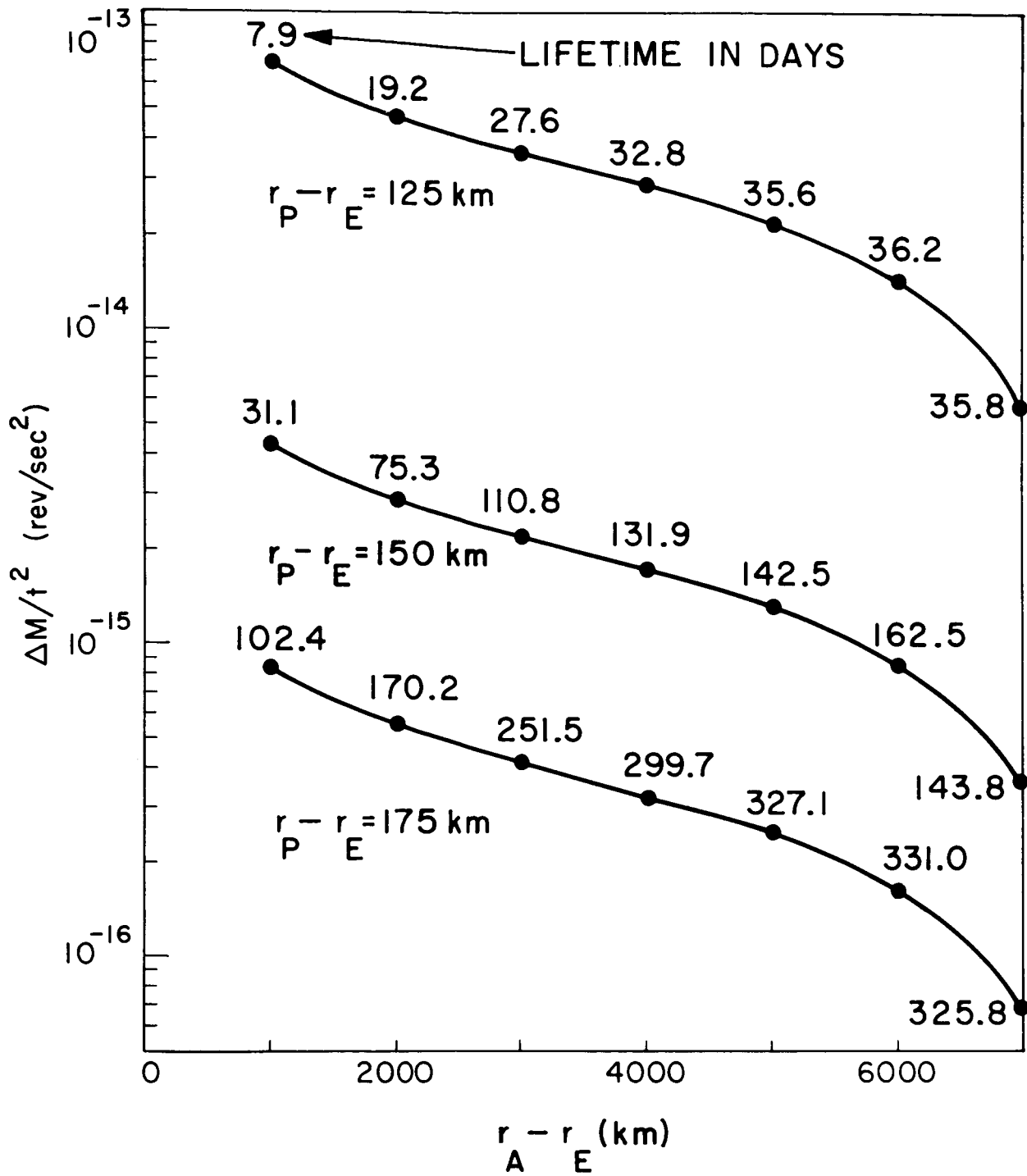


Figure 2.  $\Delta M/t^2$  versus apogee for the example of Scout-launched satellites.

A rough lower limit on the useful separation is set by the tracking accuracy; the separation should be many times greater than 2 arcsec as seen from the earth's surface. A hazy upper limit corresponds to a separation so great that the satellites are no longer in nearly identical orbits. The film dimension of the Baker-Nunn camera (30° topocentric) provides an alternative limit that might be adopted if both satellites were to appear on the same film; this is hardly necessary, however.

Another sort of limit is imposed by the time interval available for observation. In Figure 1, satellite orbital lifetimes have been noted at intervals along the curves. The lifetimes have been estimated using the procedure described by Jacchia and Slowey (1963a). Probably, observations should be made over at least a month for a statistically sound orbit determination. For practical reasons, it may be reasonable to limit the duration of the experiment to a few months. Surely a duration greater than a year is dubious.

A specific example will illustrate the open possibilities. Suppose that the atmospheric density at 150 km is an objective and that 3 months is adopted as a reasonable duration for the experiment. From Figure 1, an apogee altitude of about 2400 km is indicated for these conditions. Also, Figure 1 gives  $[dP(2)/dt] - [dP(1)/dt] = 2.3 \times 10^{-7}$  for the initial relative rate of change of the period. From Figure 2, the spheres would separate about 0.1 rad during the first month. The separation would be some 0.4 rad after 2 months and would be something like 1.0 rad before the satellite demise after 3 months. The satellite diameters, masses, and orbital parameters for this case are given in Table 2.

This example illustrates an important characteristic of the orbits satisfying the imposed conditions — namely, they are initially quite eccentric. This is fortunate for it facilitates reliable tracking.

Table 2. Orbital parameters at apogee 2400 km

$$r_P - r_E = 150 \text{ km}$$

$$r_A - r_E = 2400 \text{ km}$$

$$a = 7653 \text{ km}$$

$$e = 0.147$$

$$m = 119.3 \text{ kg}$$

$$D(1) = 24 \text{ cm}$$

$$D(2) = 76 \text{ cm}$$

$$m(1) = 10.8 \text{ kg}$$

$$m(2) = 108.5 \text{ kg}$$

$$A/m = 0.0418 \text{ cm}^2 \text{ g}^{-1}$$

$$\text{Satellite density (1)} = 1.49 \text{ g cm}^{-3}$$

$$\text{Satellite density (2)} = 0.47 \text{ g cm}^{-3}$$

$$\text{Lifetime} = 90 \text{ days}$$

An alternative criterion for selecting a set of satellite and orbit parameters uses equation (27) with the  $t$  replaced by the lifetime of the satellite. The resulting value  $\Delta M$  is a figure of merit akin to the total separation of the satellites during their life. Using the same Scout performance data, Figure 3 shows this  $\Delta M$  as a function of apogee for the perigee altitude of 150 km. In some sense, the maximum of such a curve represents an optimum situation. The characteristics of this case are shown in Table 3.

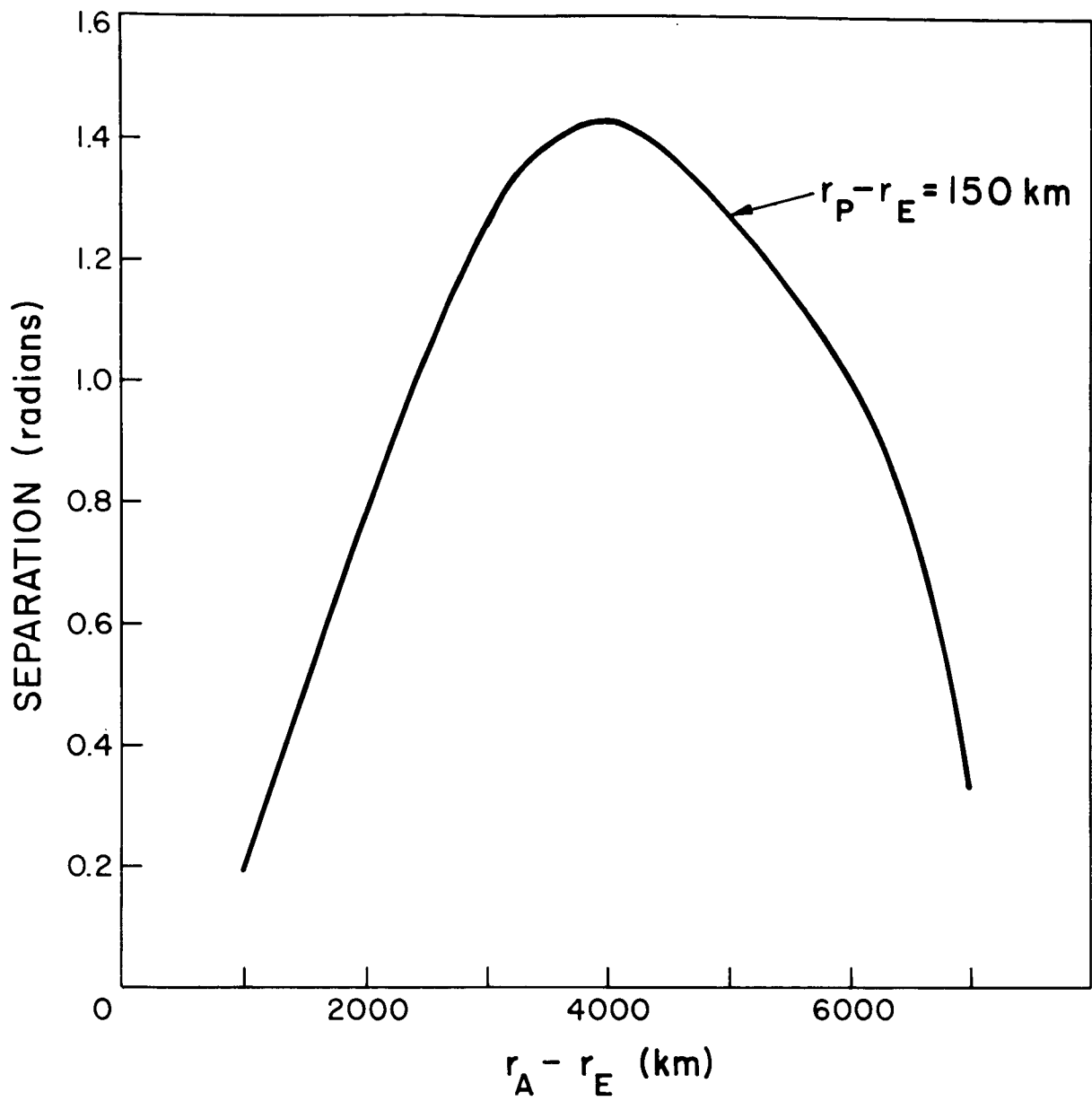


Figure 3. Separation as a function of apogee, for example of Scout-launched satellites.

Table 3. Orbital parameters at apogee 4000 km

$$r_P - r_E = 150 \text{ km}$$

$$r_A - r_E = 4000 \text{ km}$$

$$a = 8453 \text{ km}$$

$$e = 0.228$$

$$m = 99.5 \text{ kg}$$

$$D(1) = 40 \text{ cm}$$

$$D(2) = 76 \text{ cm}$$

$$m(1) = 21.9 \text{ kg}$$

$$m(2) = 77.6 \text{ kg}$$

$$A/m = 0.0573 \text{ cm}^2 \text{ g}^{-1}$$

$$\text{Satellite density (1)} = 0.654 \text{ g cm}^{-3}$$

$$\text{Satellite density (2)} = 0.338 \text{ g cm}^{-3}$$

$$\text{Lifetime} = 131.9 \text{ days}$$

## 12. EXAMPLE 2, SATURN SECONDARY EXPERIMENT

For a secondary experiment on a Saturn or another large launch vehicle, a set of nominal parameters is given in Table 4. The smallest sphere diameter again corresponds to the lower limit for reliable tracking, the largest diameter is dictated by available space within the vehicle, and the third sphere has an intermediate diameter.

Table 4. Nominal parameters for Saturn secondary experiment\*

Satellite	Diameter (m)	Mass (kg)	Density ( $\text{g cm}^{-3}$ )	A/m ( $\text{cm}^2 \text{g}^{-1}$ )
1	0.2	15	3.58	0.0209
2	0.6	135	1.19	0.0209
3	1.0	375	0.72	0.0209
4	0.6	612	5.4	0.0046

\* perigee = 160 km,  
apogee = 2000 km,  
a = 7458 km,  
 $T_b = 300^\circ \text{K}$ .

Perigee altitude is selected as an interesting region of the atmosphere. The nominal apogee altitude then corresponds to about an orbital lifetime of 6 months. The total mass of the ensemble corresponds to an estimate of vehicle payload that might be available for a secondary experiment (2500 pounds).

In Table 4, spheres 1, 2, and 3 have the same A/m. Sphere 4 has the same size as sphere 2, but a much smaller A/m. This last sphere has two purposes: detection of temporal changes of the atmosphere over an extended time interval, and examination of the adequacy of the geopotential representation.

For the first three spheres, the relative rates of change in the period given by equation (12) are shown in Figure 4. Curves are given for a family of perigee and apogee values in the neighborhood of the nominal orbit in Table 4.

For the cases in Figure 4, Figure 5 gives the corresponding coefficients of  $t^2$  in equation (27). In Figures 6 and 7, the separation of the spheres as a function of time is illustrated for an apogee of 2000 km and various perigees.

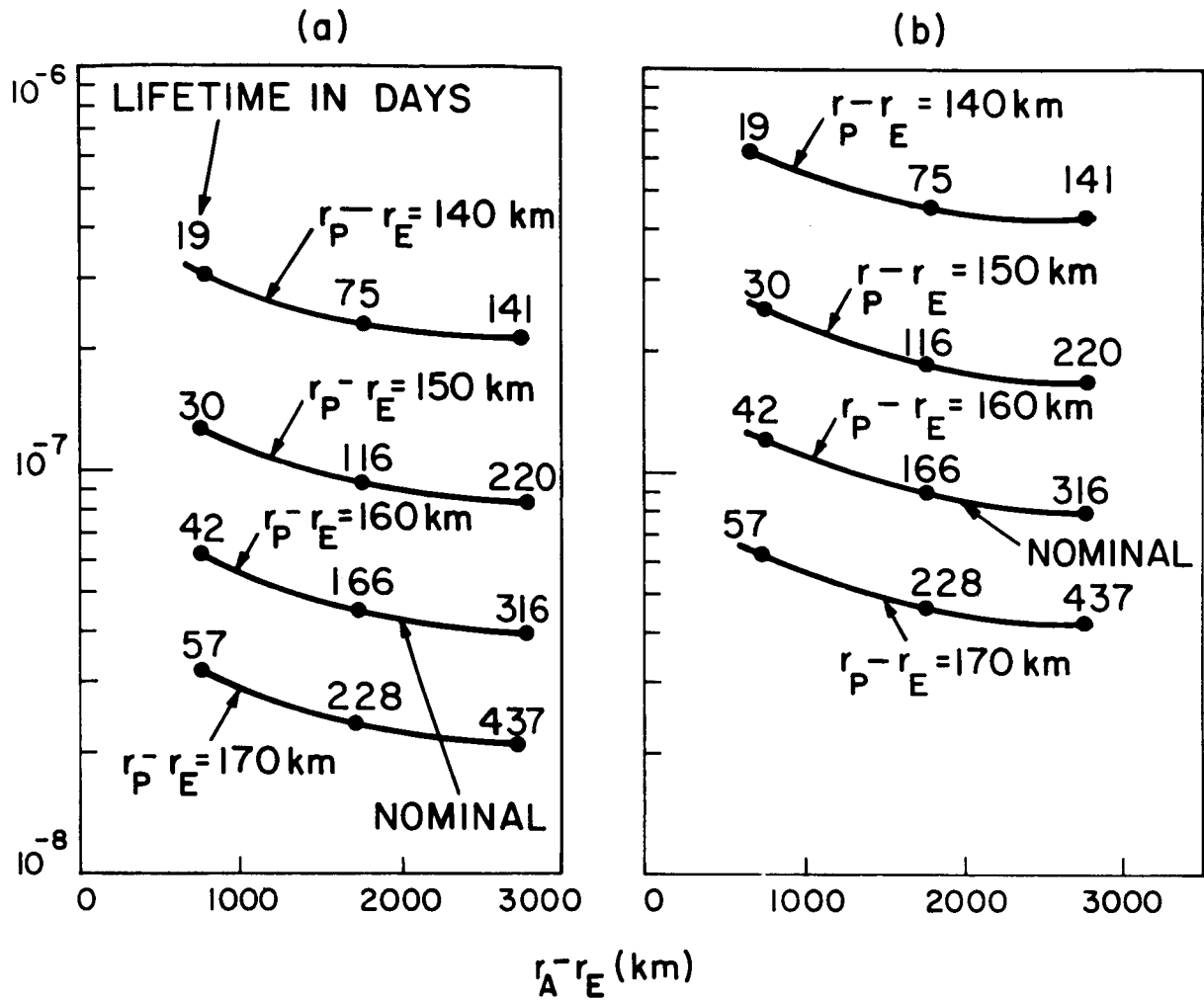


Figure 4. (a)  $\frac{dP(2)}{dt} - \frac{dP(1)}{dt}$  versus apogee for the example of Saturn-launched satellites.

(b)  $\frac{dP(3)}{dt} - \frac{dP(1)}{dt}$  versus apogee for the example of Saturn-launched satellites.  $D(1) = 20$  cm;  $D(2) = 60$  cm;  $D(3) = 100$  cm.

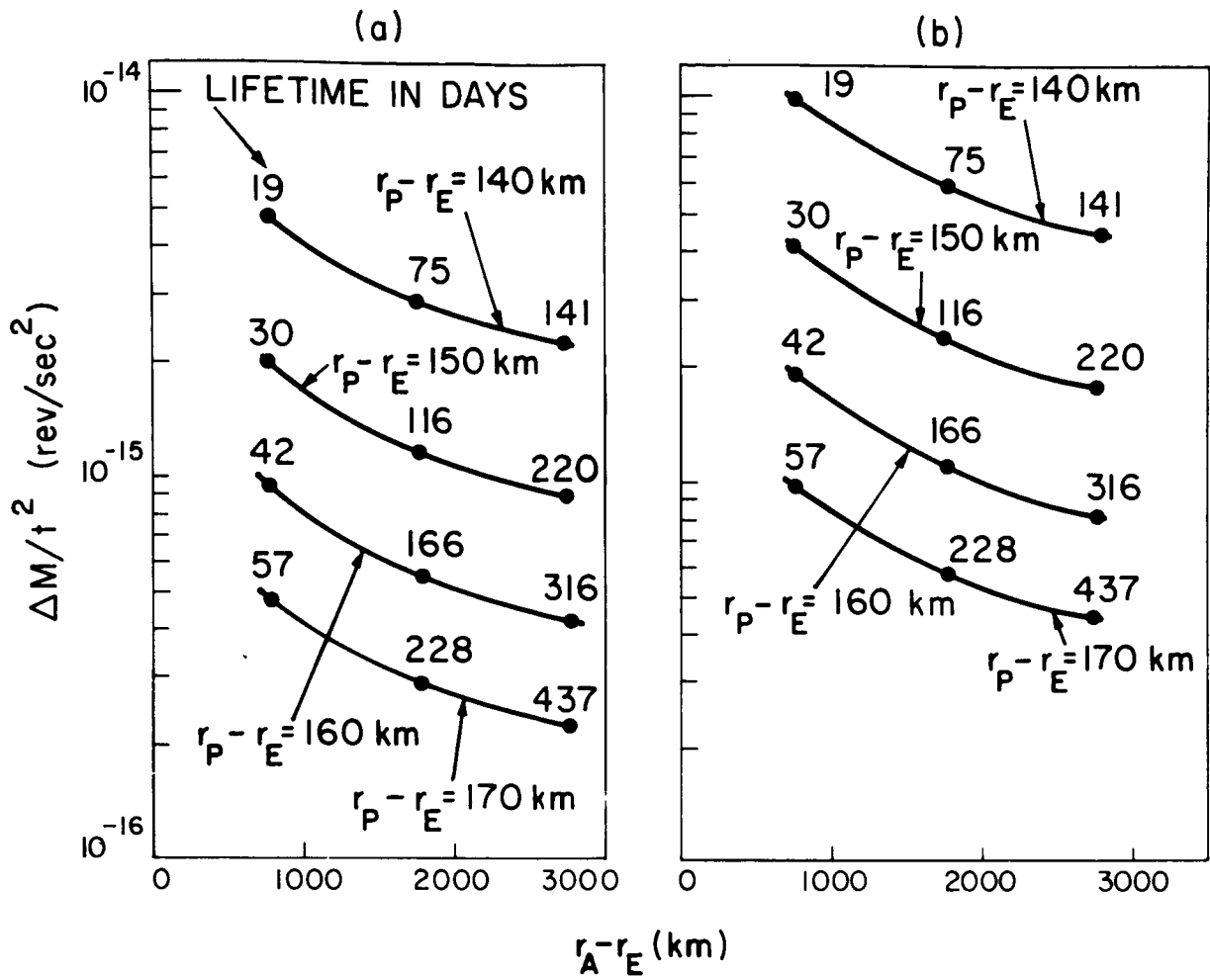


Figure 5. Curves for the example of Saturn-launched satellites.  
 $\frac{\Delta M}{t^2}$  versus apogee for: (a) sphere 2 from sphere 1, and (b) sphere 3 from sphere 1.

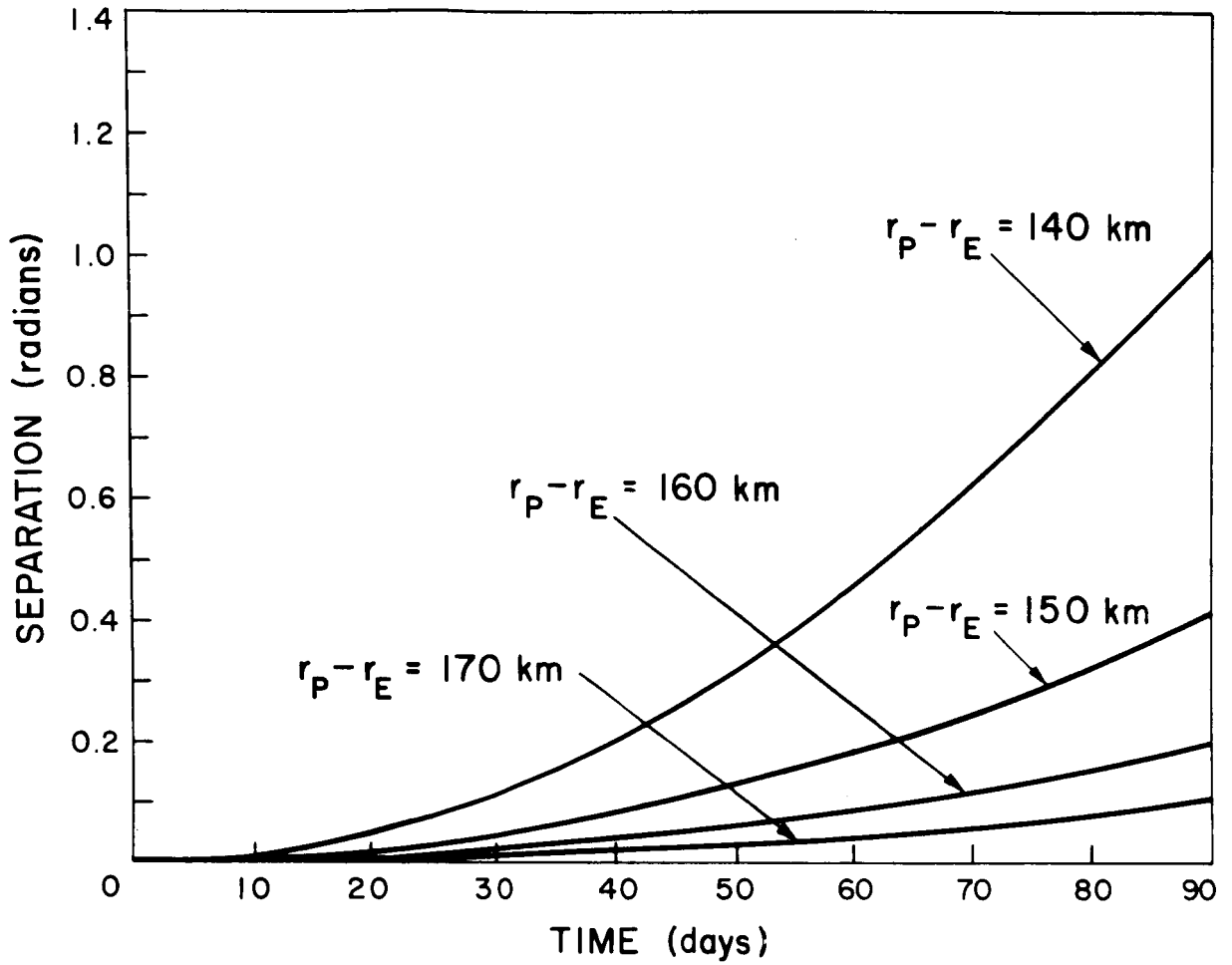


Figure 6. Angular separation of sphere 2 from sphere 1 at apogee 2000 km versus time, for Saturn-launched satellites.

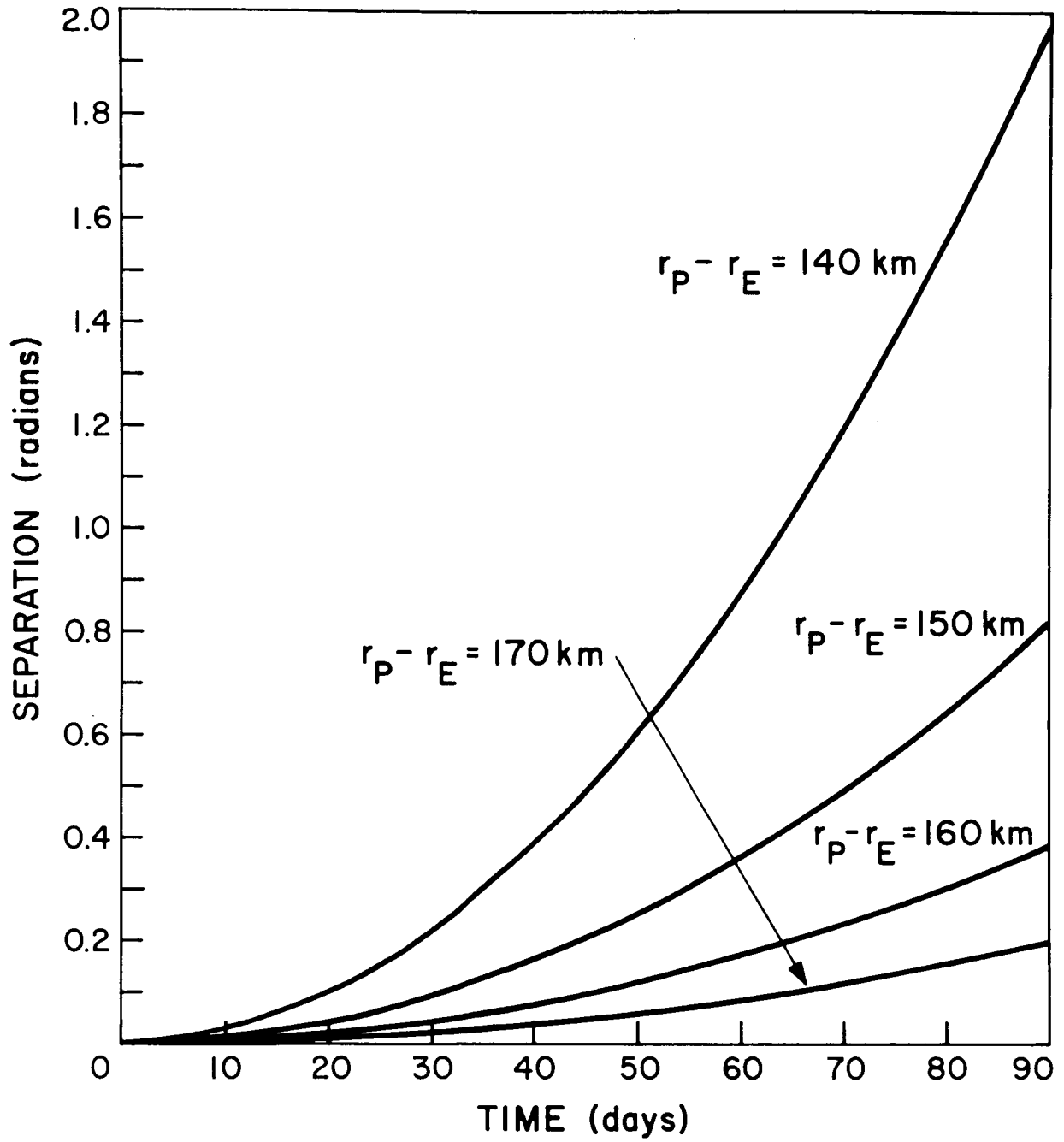


Figure 7. Angular separation of sphere 3 from sphere 1 at apogee 2000 km versus time, for Saturn-launched satellites.

### 13. CONCLUSIONS

In summary, an interesting class of experiments can be defined that achieve a dual objective. They measure the atmospheric density in the altitude range sometimes referred to as the "ignorosphere," and they provide an experimental check on the theory of near-free-molecule-flow aerodynamics.

The means for collecting the observational data are completely in existence in the SAO network of Baker-Nunn cameras. The data-analysis techniques are closely analogous to proved procedures used already to obtain much of the present knowledge of the atmosphere above 200 km.

The launch-vehicle requirements are minimal for a satellite experiment. The Scout vehicle can accommodate a useful experiment. The complexity of the payload is also minimal, which makes the experiment attractive for a secondary payload on a launch vehicle. An ensemble of spherical satellites can be specified for more or less ambitious investigations, depending on the available vehicle capacity.

#### 14. REFERENCES

COOK, G. E.

1965. Satellite drag coefficients. *Planet. Space Sci.*, vol. 13, pp. 929-946.

GAPOSCHKIN, E. M.

- 1966a. Tesseral harmonic coefficients and station coordinates from the dynamic method. *Smithsonian Astrophys. Obs. Spec. Rep. No. 200*, vol. 2, pp. 105-257.
- 1966b. Orbit determination. *Smithsonian Astrophys. Obs. Spec. Rep. No. 200*, vol. 1, pp. 77-183.
1967. A dynamical solution for the tesseral harmonics of the geopotential and station coordinates using Baker-Nunn data. In *Proceedings 7th International COSPAR Space Science Symposium*, North-Holland Publ. Co., Amsterdam, in press.

HELLER, G.

1961. Thermal environment and control of space vehicles. In *Handbook of Astronautical Engineering*, ed. by H. H. Koelle, McGraw-Hill Book Co., New York, pp. 22-104 to 22-123.

JACCHIA, L. G.

1963. Variations in the earth's upper atmosphere as revealed by satellite drag. *Rev. Mod. Phys.*, vol. 35, pp. 973-991.
1965. Static diffusion models of the upper atmosphere with empirical temperature profiles. *Smithsonian Contr. Astrophys.*, vol. 8, no. 8, pp. 215-257.

JACCHIA, L. G., AND SLOWEY, J.

- 1963a. Formulae and tables for the computation of lifetimes of artificial satellites. *Smithsonian Astrophys. Obs. Spec. Rep. No. 135*, 23 pp.
- 1963b. Accurate drag determinations for eight artificial satellites; atmospheric densities and temperatures. *Smithsonian Contr. Astrophys.*, vol. 8, no. 1, pp. 1-99.

JACOBS, R. L.

1967. Atmospheric density derived from the drag of eleven low-altitude satellites. *Journ. Geophys. Res.*, vol. 72, pp. 1571-1581.

KÖHNLEIN, W.

1966. Combination of geometric and dynamic results. *Smithsonian Astrophys. Obs. Spec. Rep. No. 200*, vol. 2, pp. 259-299.
1967. Corrections to station coordinates and to nonzonal harmonics from Baker-Nunn observations. In *Proceedings 7th International COSPAR Space Science Symposium*, North-Holland Publ. Co., Amsterdam, in press.

KOZAI, Y.

1964. New determination of zonal harmonics coefficients of the earth's gravitational potential. *Publ. Astron. Soc. Japan*, vol. 16, pp. 263-284; also in *Smithsonian Astrophys. Obs. Spec. Rep. No. 165*, 38 pp., 1964.
1966. The earth gravitational potential derived from satellite motion. *Space Sci. Rev.*, vol. 5, pp. 818-879.

LUNDQUIST, C. A.

1967. Procedures for a near-free-molecule-flow aerodynamics experiment. Presented at Amer. Chem. Soc.-Amer. Phys. Soc. Joint Section Meeting, March 17-18, Hartford, Connecticut. (Abstract in *Bull. Amer. Phys. Soc.*, 1967, in press.)

LUNDQUIST, C. A., AND VEIS, G., eds.

1966. Geodetic Parameters for a 1966 Smithsonian Institution Standard Earth. *Smithsonian Astrophys. Obs. Spec. Rep. No. 200*, 3 vols., 686 pp.

MASLACH, G. J., WILLIS, D. R., TANG, S., AND KO, D.

1964. Recent experimental and theoretical extensions of nearly free molecular flow. In *Fourth International Symposium on Rarefied Gas Dynamics*, Toronto, Canada.

NATIONAL AERONAUTICS AND SPACE ADMINISTRATION

1966. Performance and flight planning. *Scout User's Manual*, vol. 5, 74 pp.

SCHAAF, S. A., AND CHAMBRÉ, P. L.

1958. Flow of rarefied gases. High Speed Aerodynamics and Jet Propulsion, vol. 4, Part G, Section H. 8, Princeton Univ. Press, Princeton, New Jersey.

SHERMAN, F. S., WILLIS, D. R., AND MASLACH, G. J.

1964. Nearly free molecular flow, a comparison of theory and experiment. In Applied Mechanics, Proceedings of the Eleventh International Congress of Applied Mechanics, ed. by H. Görtler, Munich, pp. 871-877.

SPRINGER, G. S., AND TSAI, S. W.

1964. Effect of thermal accommodation on cylinder and sphere drag in free molecule flow. AIAA Journ., vol. 2, pp. 126-128.

STERNE, T. E.

1958. An atmospheric model, and some remarks on the inference of density from the orbit of a close earth satellite. Astron. Journ., vol. 63, no. 3, pp. 81-87.

VEIS, G.

1965. Illumination and visibilities of satellites. COSPAR Information Bulletin No. 25, p. 13.

VEIS, G., AND MOORE, C. H.

1960. Smithsonian Astrophysical Observatory differential orbit improvement program. In Astronautics Information, Seminar Proceedings, Tracking Programs and Orbit Determination, Jet Propulsion Laboratory, Pasadena, California, p. 165.

WACHMAN, H. Y.

1962. The thermal accommodation coefficient: a critical survey. ARS Journ., vol. 32, pp. 2-12.

ZIRKER, J. B., WHIPPLE, F. L., AND DAVIS, R. J.

1958. Time available for the optical observation of an earth satellite. In Scientific Uses of Earth Satellites, 2nd rev. ed., ed. by J. A. van Allen, Univ. of Michigan Press, Ann Arbor, pp. 23-28.

## BIOGRAPHICAL NOTES

LOUISA S. LAM received her BA in Mathematics from Wellesley College in 1965, and is currently working toward an MS in Mathematics at the University of Toronto.

She was a Research Assistant to Dr. Charles A. Lundquist at Smithsonian Astrophysical Observatory from June 1965 until September 1966.

GERALDINE M. MENDES received her AB in Physics from Northeastern University in 1963, and expects to receive her MS in Physics from that university in 1969.

From March 1964 to May 1967, she was a mathematician in the Data Division of the Smithsonian Astrophysical Observatory. Currently she is a mathematician in the Research and Analysis Division, where she is assigned primarily to the Standard Earth program.

CHARLES A. LUNDQUIST joined the Smithsonian Astrophysical Observatory as Assistant Director for Science in 1962. In this position, he is responsible for organizing and coordinating current research projects, as well as seeking new directions for future research.

From 1956 to 1960 he was Chief of the Physics and Astrophysics Section, Research Projects Laboratory, Army Ballistic Missile Agency; and from 1960 to 1962 he held concurrent positions as Director of the Supporting Research Office, and Chief of the Physics and Astrophysics Branch of the Research Projects Division at the Marshall Space Flight Center.

Dr. Lundquist received his undergraduate degree from South Dakota State College in 1949, and his doctorate in 1954 from the University of Kansas.

His own research includes various topics in space science.

## NOTICE

This series of Special Reports was instituted under the supervision of Dr. F. L. Whipple, Director of the Astrophysical Observatory of the Smithsonian Institution, shortly after the launching of the first artificial earth satellite on October 4, 1957. Contributions come from the Staff of the Observatory.

First issued to ensure the immediate dissemination of data for satellite tracking, the reports have continued to provide a rapid distribution of catalogs of satellite observations, orbital information, and preliminary results of data analyses prior to formal publication in the appropriate journals. The Reports are also used extensively for the rapid publication of preliminary or special results in other fields of astrophysics.

The Reports are regularly distributed to all institutions participating in the U. S. space research program and to individual scientists who request them from the Publications Division, Distribution Section, Smithsonian Astrophysical Observatory, Cambridge, Massachusetts 02138.